Unraveling the Structure of Λ Hyperons with Polarized $\Lambda\bar{\Lambda}$ Pairs

M. Ablikim *et al.*[*]
(BESIII Collaboration)

(Received 13 June 2025; revised 5 September 2025; accepted 12 September 2025; published 4 November 2025)

With data collected in a dedicated energy scan from 2.3864 up to 3.0800 GeV, the BESIII Collaboration provides the first complete energy-dependent measurements of the Λ electromagnetic form factors in the timelike region. By combining double-tag and single-tag events from the $e^+e^- \to \Lambda\bar{\Lambda} \to p\pi^-\bar{p}\pi^+$ reaction, we achieve a complete decomposition of the spin structure of the reaction at five energy points, with high statistical and systematic precision. Our data reveal that while the modulus of the ratio between the electric and magnetic form factor, $R(q^2) = |G_E(q^2)/G_M(q^2)|$, remains fairly constant across the considered energy range, the relative phase $\Delta\Phi(q^2) = \Phi_E(q^2) - \Phi_M(q^2)$ changes by more than 90° between 2.396 and 2.6544 GeV. Using a fit to our data based on dispersion relations, the complex form factor ratio is determined as a function of q^2, and the preferred solution has multiple zero-crossings in the complex plane. From the derivative of the ratio at $q^2 = 0$, the root-mean-squared charge radius of the Λ is obtained. The two most probable solutions yield a negative root-mean-squared charge radius, indicating an asymmetric charge distribution where the *ds* quark pair lies close to the center of the Λ hyperon.

DOI: 10.1103/9f1h-fl4k

To understand how almost massless quarks form massive hadrons is a challenging endeavor, involving the full complexity of the strong interaction and its emergent phenomena. Electromagnetic form factors (EMFFs) provide a powerful tool to study the strong interaction. Probed in virtual photon-hadron processes, EMFFs quantify hadron structure in terms of analytic functions of the squared four-momentum transfer q^2 carried by the photon. More than 70 years of detailed investigations employing elastic electron-proton scattering have unraveled the spatial distribution and motion of quarks and gluons inside the proton [1,2]. In particular, the electric form factor constitutes an instrument to determine the charge radius, complementary to atomic spectroscopy methods [3]. Possible EMFF sign changes, or *zero-crossings*, at high q^2, are governed by the momentum dependence of the running strong coupling and mass functions of the quarks inside the hadron [4,5]. Such zero-crossings are predicted for nucleons by Dyson-Schwinger calculations but are not yet experimentally established [6]. While neutron data elucidate the *u-d* quark flavor dependence [7], the impact of the ≈20 times heavier strange *s* quark remains rather uncharted territory. Addressing this question is challenging since the short lifetime (10^{-10} s) of strange *hyperons* makes them virtually unfeasible for elastic electron-hadron scattering experiments—the only existing measurement of this kind is for the Σ^- hyperon [8]. However, *timelike* EMFFs of hyperons can be accessed through the process $e^+e^- \to \gamma^* \to Y\bar{Y}$, where Y ($\bar{Y}$) denotes a hyperon (antihyperon). Whereas spacelike ($q^2 = -Q^2 < 0$) EMFFs are real, the timelike ($q^2 > 0$) ones are complex with a phase reflecting the fact that the virtual photon can undergo quantum fluctuations into an intermediate multihadron state, e.g., 2π or 3π [9].

For spin 1/2 baryons, the relative phase between the electric and magnetic form factors manifests itself in transversely polarized final-state baryons and antibaryons, even for an unpolarized initial state [10]. Here, ground-state hyperons have an advantage over nucleons: their weak, self-analyzing decays offer straightforward access to their polarization. This was exploited by BESIII in a pioneering measurement of the EMFF phase of the Λ hyperon, obtaining the complete EMFFs at a single energy for the first time [11]. This led to increased activity in the theory community with a variety of approaches: $\Lambda\bar{\Lambda}$ final state interactions [12], vector meson dominance [13], covariant spectator model [14], and dispersive calculations [9,15]. In Ref. [9], Mangoni *et al.* outlined a method to study zero-crossings and even determine the charge root-mean-squared (rms) radius $\bar{r}_E^{\Lambda}$ of the Λ by combining the BESIII measurement [11] with a partial EMFF determination at two energy points by *BABAR* [16]. However, the scarcity of data resulted in a highly ambiguous solution.

[*]Full author list given at the end of the Letter.

TABLE I. c.m.s. energies (in GeV), integrated luminosities $\mathcal{L}$ (in pb^{-1}), ISR + VP corrections $(1+\delta)$, background subtracted yields N, efficiencies ϵ (in %), and the resulting Born cross sections (in pb) with statistical and systematic uncertainties. For the single-tag efficiencies $\epsilon_{1,\Lambda}$, $\epsilon_{2,\Lambda}$, $\epsilon_{1,\bar{\Lambda}}$, and $\epsilon_{2,\bar{\Lambda}}$, 1 and 2 refer to the charged and neutral decay modes, respectively, of the untagged decay.

Energy	$\mathcal{L}$	$(1+\delta)$	$N_{\Lambda\bar{\Lambda}}$	$N_{\bar{\Lambda}}$	N_{Λ}	$\epsilon_{\Lambda\bar{\Lambda}}$	$\epsilon_{1,\bar{\Lambda}}$	$\epsilon_{2,\bar{\Lambda}}$	$\epsilon_{1,\Lambda}$	$\epsilon_{2,\Lambda}$	σ_B
2.3864	22.6	0.98	227 ± 15	373 ± 19	315 ± 20	18.6	12.3	31.8	11.7	28.2	132.7(45)(28)
2.3960	66.9	0.99	596 ± 24	973 ± 32	575 ± 25	18.5	12.1	31.4	7.5	18.4	120.2(26)(25)
2.6544	67.8	1.23	224 ± 15	300 ± 18	244 ± 17	21.7	9.7	31.2	9.0	27.7	31.0(11)(07)
2.9000	105.5	1.57	117 ± 11	120 ± 11	108 ± 11	19.1	6.5	23.5	6.2	22.0	8.7(05)(03)
2.9500	16.0	1.65	16 ± 4	12 ± 4	14 ± 4	17.4	6.4	23.8	6.1	21.9	7.2(11)(02)
2.9810	16.0	1.71	16 ± 4	13 ± 4	13 ± 4	18.8	5.9	22.9	5.6	21.5	7.7(12)(02)
3.0000	15.8	1.75	13 ± 3	12 ± 4	14 ± 4	12.9	6.2	23.2	5.9	21.6	7.1(12)(02)
3.0200	17.3	1.75	11 ± 3	12 ± 4	14 ± 4	14.1	6.1	23.8	5.8	22.2	5.6(10)(02)
3.0800	126.6	1.85	65 ± 8	60 ± 8	62 ± 8	14.8	4.1	16.1	3.9	15.1	4.6(04)(02)

Energy-dependent phase measurements are expected to constrain the calculations and improve the Λ charge rms radius determination.

A dedicated energy scan at center-of-mass system (c.m.s.) energies between 2.0 and 3.08 GeV was performed in 2014–2015 at BESIII. At these energies, we expect the influence from vector charmonium resonances to be negligible and the production mechanism to be dominated by one-photon exchange. Each energy corresponds to a q^2 through the relation $E^2_{c.m.s.}/c^2 = q^2$. From the resulting rich data, partial EMFF information has been obtained for protons [17], neutrons [18,19], Σ [20–22], and Ξ [23–25]. Furthermore, exclusive double-tag analyses of the $e^+e^- \to \Lambda\bar{\Lambda} \to p\pi^-\bar{p}\pi^+$ and $e^+e^- \to \Sigma^+\bar{\Sigma}^- \to p\pi^0\bar{p}\pi^0$ reactions enabled the complete determination of the EMFF for Λ at one energy [11] and for Σ^+ at two energies [26]. In this Letter, we combine the analysis of double-tag $e^+e^- \to \Lambda\bar{\Lambda} \to p\pi^-\bar{p}\pi^+$ with single-tag $e^+e^- \to \Lambda X \to p\pi^- X$ and $e^+e^- \to \bar{\Lambda} X \to \bar{p}\pi^+ X$ at five different energies. This enables the complete determination of the Λ EMFF at five energies within the range 2.3864–3.0800 GeV. In addition, we measure the production cross section at nine energies. The integrated luminosities at all c.m.s. energies are listed in Table I.

The Beijing Spectrometer (BESIII, [27]) at the Beijing Electron Positron Collider is uniquely suitable for hyperon EMFF investigations. The BESIII detector covers 93% of the 4π solid angle and is comprised of a small-cell, helium-based multilayer drift chamber (MDC) for tracking; a time-of-flight (TOF) system based on plastic scintillators; an electromagnetic calorimeter made of CsI(Tl) crystals; a muon counter made of resistive plate chambers; and a superconducting solenoid magnet with a central field of 1.0 T.

To determine the modulus of the form factor ratio $R(q^2) = |G_E(q^2)/G_M(q^2)|$ and the relative phase $\Delta\Phi(q^2) = \Phi_E(q^2) - \Phi_M(q^2) = \arg[G_E(q^2)/G_M(q^2)]$, we apply the formalism outlined in Ref. [28]. The double-tag analysis gives access to five independent angles: the Λ scattering angle (θ) in the e^+e^- c.m.s. system, and the helicity angles θ_1 and ϕ_1 (θ_2 and ϕ_2), defined as the polar and azimuthal angle of the proton (antiproton) in the helicity frame of the mother Λ ($\bar{\Lambda}$). In the single-tag case, the helicity angles of the untagged hyperon are integrated out, and by defining the angle θ_p between the proton (antiproton) and the normal of the Λ ($\bar{\Lambda}$) scattering plane [29], Eqs. (6.55) and (6.56) in Ref. [28] can be simplified to

$$\mathcal{W}(R, \Delta\Phi, \theta, \theta_p) = 1 + \frac{\tau - R^2}{\tau + R^2}\cos^2\theta + \alpha\sqrt{1 - \left[\frac{\tau - R^2}{\tau + R^2}\right]^2}\,\sin\Delta\Phi\,\sin\theta\,\cos\theta\,\cos\theta_p, \quad (1)$$

where $\mathcal{W}(R, \Delta\Phi, \theta, \theta_p)$ is the joint decay distribution, $\tau = (q^2/4m_\Lambda^2)$, and α is the Λ decay asymmetry parameter. The latter has been measured by BESIII [30–33] and CLAS [34]. Owing to the numerous new measurements, the Particle Data Group (PDG) [35] continuously updates the world average. For this Letter, we adopt the current average $\langle\alpha\rangle = (\alpha - \bar{\alpha})/2$ from the BESIII measurements [30–33], $\alpha = 0.754$, assuming CP symmetry, i.e., $\alpha = -\bar{\alpha}$. This allows one to include measurements of $\bar{\alpha}$ for increased precision. The resulting value differs from the latest PDG value only on the subpercent level, which is well beyond the precision of our phase measurement.

Detection efficiencies have been obtained from Monte Carlo (MC) simulations. The Continuum Exclusive generator (ConExc), incorporating initial state radiation (ISR) and vacuum polarization (VP) effects [36], has been employed to generate 100 000 signal events at each energy, including the decay modes $\Lambda \to p\pi^- + \text{c.c.}$

and $\Lambda \to n\pi^0$ + c.c. The background is studied using the inclusive process $e^+e^- \to q\bar{q}$ at 2.396 GeV, where the generated 2.86 M events correspond to an integrated luminosity of 45 nb^{-1}. In addition, samples of 100 000 events with the most prominent background channel $e^+e^- \to \Lambda\bar{\Sigma}^0$ + c.c. are generated at all c.m.s. energies. The normalization factors used in the $R(q^2)$ and $\Delta\Phi(q^2)$ parameter estimation are obtained using 5 M phase-space signal events at each energy. Systematic checks are performed using a BESIII adaptation of EvtGen [37], describing the full angular distribution from Ref. [28].

In the event selection, the point of closest approach of charged tracks to the interaction point must be inside a cylindrical volume defined by the radial distance $V_{xy} \leq 10$ cm and the longitudinal distance $V_z \leq 30$ cm from the interaction point. The z axis is the symmetry axis of the MDC, and the polar angle with respect to the z axis must fulfill $|\cos\theta_{\rm lab}| \leq 0.93$. Furthermore, we require $p\pi^-$ and $\bar{p}\pi^+$ combinations to have good vertex fits for production and decay, which determine the decay length L as the distance between the two vertices. The production vertex position, measured independently using Bhabha scattering to a precision of a few hundred μm, is used as a constraint in the vertex fit. If more than one combination exists in an event, we select the one giving the largest L. This requirement selects the long-lived $\Lambda/\bar{\Lambda}$ while rejecting random or nonresonant $p\pi^-$ and $\bar{p}\pi^+$ combinations. The events are organized into three independent categories, referred to as double-tag $\Lambda\bar{\Lambda}$, single-tag Λ, and single-tag $\bar{\Lambda}$. The double-tag $\Lambda\bar{\Lambda}$ selection is essentially the same as in Ref. [11], but with complete particle identification (PID) of protons, antiprotons, and pions, using TOF and dE/dx information from the MDC. The χ^2_{4C} of a four-constraint ($4C$) kinematic fit, exploiting four-momentum conservation of the $e^+e^- \to p\pi^-\bar{p}\pi^+$ process, must be less than 130. Finally, the $p\pi^-$ and $\bar{p}\pi^+$ combinations must satisfy $|M(p\pi) - m_\Lambda| \leq 6$ MeV/c^2 which corresponds to $\pm 4\sigma$ of the peak in the $p\pi$ invariant mass spectrum. These criteria give efficiencies within the range of (13–22)% (see $\epsilon_{\Lambda\bar{\Lambda}}$ in Table I) and a background fraction of less than 1%.

In the single-tag selection, we apply the same criteria on V_{xy}, V_z, $\cos\theta_{\rm lab}$, PID, and good vertex fits as for double-tag. In addition, we require the decay length significance $L/\Delta L$ to be larger than 0. To exclude events containing Λ or $\bar{\Lambda}$ that do not come from the two-body $e^+e^- \to \Lambda\bar{\Lambda}$ process, we require the magnitude of the $\Lambda/\bar{\Lambda}$ momentum in the c.m.s. system, p_Λ, to be within a $\pm 3\sigma$ window around the predicted value for each energy; at 2.396 GeV, we require $|p(p\pi) - p_\Lambda| \leq 14.1$ MeV/c. Since the background yield is larger in the single-tag case, we use a tighter invariant mass criterion: $|M(p\pi) - m_\Lambda| \leq 4.7$ MeV/c^2. In the single-tag Λ case, additional background arises due to protons from secondary interactions with the beam pipe. To eliminate these events, we require the sum of the χ^2 of the production and decay vertex fits to satisfy $\chi^2_{\rm prod} + \chi^2_{\rm decay} \leq 8$ and $|L/\Delta L| \leq 30$. Events containing both good $\Lambda \to p\pi^-$ and $\bar{\Lambda} \to \bar{p}\pi^+$ tags are not included, as they are in the double-tag sample.

For single-tag events, we do not exploit information from the untagged $\Lambda/\bar{\Lambda}$, decaying either *via* the charged mode or through the neutral $\Lambda \to n\pi^0/\bar{\Lambda} \to \bar{n}\pi^0$. The efficiencies for the single-tag modes, denoted $\epsilon_{1,\Lambda}$, $\epsilon_{2,\Lambda}$, $\epsilon_{1,\bar{\Lambda}}$, and $\epsilon_{2,\bar{\Lambda}}$, where 1 refers to the charged mode and 2 to the neutral one, are listed in Table I. We note that the efficiencies $\epsilon_{2,\Lambda}$ and $\epsilon_{2,\bar{\Lambda}}$ are larger since there is no overlap with the double-tag sample. The background, estimated using the $M(p\pi^-)$ and $M(\bar{p}\pi^+)$ sidebands (see Ref. [38]), is found to be $\leq 1.5\%$ and $\leq 0.5\%$ for single-tag Λ and single-tag $\bar{\Lambda}$, respectively. The small background in both double-tag and single-tag data samples is confirmed in simulations of the inclusive $e^+e^- \to q\bar{q}$ process and reactions with similar topology, e.g., $e^+e^- \to \Lambda\bar{\Sigma}^0$ + c.c.

The Born cross section $\sigma_B(e^+e^- \to \gamma^* \to \Lambda\bar{\Lambda})$ is first calculated for the double-tag $\Lambda\bar{\Lambda}$, single-tag Λ, and single-tag $\bar{\Lambda}$ samples separately. For the double-tag case, we use

$$\sigma_B = \frac{\sigma_{\rm exp}}{1+\delta} = \frac{N_{\Lambda\bar{\Lambda}}}{\mathcal{L}(1+\delta)\epsilon_{\Lambda\bar{\Lambda}}\mathcal{B}_1^2}, \tag{2}$$

where $N_{\Lambda\bar{\Lambda}}$ is obtained with the two-dimensional sideband method presented in Ref. [39], $\mathcal{L}$ is the integrated luminosity as given in Table I, $\epsilon_{\Lambda\bar{\Lambda}}$ is the efficiency, $(1+\delta)$ is the ISR and VP correction factor, and $\mathcal{B}_1 = \mathcal{B}(\Lambda \to p\pi^-) = \mathcal{B}(\bar{\Lambda} \to \bar{p}\pi^+) = 63.9 \pm 0.5\%$ and is the branching fraction from the PDG. From the single-tag Λ sample, σ_B is calculated using

$$\sigma_B = \frac{\sigma_{\rm exp}}{1+\delta} = \frac{N_\Lambda}{\mathcal{L}(1+\delta)\mathcal{B}_1(\epsilon_{1,\Lambda}\mathcal{B}_1 + \epsilon_{2,\Lambda}\mathcal{B}_2)}, \tag{3}$$

where $\mathcal{B}_2 = \mathcal{B}(\Lambda \to n\pi^0) = 35.8 \pm 0.5\%$ [35]. The number of single-tag Λ events N_Λ is determined by sideband subtraction [38]. For single-tag $\bar{\Lambda}$, we replace $N_\Lambda \to N_{\bar{\Lambda}}$, $\epsilon_{1,\Lambda} \to \epsilon_{1,\bar{\Lambda}}$ and $\epsilon_{2,\Lambda} \to \epsilon_{2,\bar{\Lambda}}$ in Eq. (3) and assume $\mathcal{B}(\Lambda \to n\pi^0) = \mathcal{B}(\bar{\Lambda} \to \bar{n}\pi^0)$.

The ISR and VP correction factors are obtained from ConExc in an iterative procedure where the input line shape of the initial step is obtained by applying a pQCD model [40] to data from *BABAR* [16] and BESIII [41]. Applying the resulting correction factors to our data, we perform a new fit using a dipole model [29]. The resulting refined line shape is used as input in the next step. This procedure is repeated until the difference between the last two iterations becomes negligible compared to other uncertainties. The cross sections obtained for the three independent samples (double tag $\Lambda\bar{\Lambda}$, single tag Λ and single tag $\bar{\Lambda}$) all agree within the statistical uncertainty and are combined using the weighted mean. The results are listed in Table I.

TABLE II. The measured $G_{\rm eff}$, the ratio $R = |G_E/G_M|$, and the relative phase $\Delta\Phi$ at each c.m.s. energy (GeV). The first uncertainty is statistical, and the second is systematic.

Energy	$G_{\rm eff}$	R	$\Delta\Phi$ (°)
2.3864	0.1307(22)(14)	1.08(15)(03)	37(12)(01)
2.3960	0.1233(13)(13)	0.91(08)(02)	42(10)(02)
2.6454	0.0586(10)(07)	1.06(16)(03)	147(13)(01)
2.9000	0.0319(09)(06)	1.04(25)(03)	148(19)(01)
2.9500	0.0295(22)(04)	···	···
2.9810	0.0305(22)(04)	···	···
3.0000	0.0294(25)(04)	···	···
3.0200	0.0262(23)(05)	···	···
3.0800	0.0240(10)(05)	0.67(33)(03)	80(69)(02)

General systematic effects arise from the luminosity (1% at each energy point [42]) and $\mathcal{B}_{1,2}$ [35]. Systematic uncertainties specific to this analysis are evaluated for the relatively large samples at 2.396 and 2.9 GeV [29], while obtained by linear interpolation or extrapolation in the remaining data points. Our analysis reveals small but non-negligible effects from differences at the subpercent level in the result when varying the $\chi^2_{\rm 4C}$ (double-tag) and $\Lambda/\bar{\Lambda}$ momentum (single-tag) selection requirements. In addition, there is a small uncertainty of (0.1–0.8)% in the $\Lambda/\bar{\Lambda}$ reconstruction efficiency and above 2.9 GeV, a contribution of (0.5–1.2)% from the $\Lambda\bar{\Sigma}^0$ background. The uncertainty from the ISR and VP corrections was evaluated by using a pQCD fit for the cross section line shape. The difference between the dipole and pQCD model results, (0.1–0.6)%, is quoted as the uncertainty. Since the MC data used for the efficiency correction are generated with an angular distribution governed by R, the uncertainty in the input parameter R will propagate to the cross section. For energies above 2.9 GeV, this uncertainty is fairly large, i.e., (2.2–2.8)%, while only within (0.6–1.4)% below 2.9 GeV. The total systematic uncertainty is well below the statistical uncertainty in all data points except at 2.396 GeV, where it is of similar magnitude; see Table I.

Assuming that the dominant process is the one-photon exchange ($e^+e^- \to \gamma^* \to \Lambda\bar{\Lambda}$), the effective form factor $G_{\rm eff}(q^2)$ can be calculated:

$$|G_{\rm eff}(q^2)| \equiv \sqrt{\frac{\sigma_B(q^2)}{\left(1+\frac{1}{2\tau}\right)\left(\frac{4\pi\alpha^2_{\rm EM}\beta}{3q^2}\right)}}. \quad (4)$$

Here, $\alpha_{\rm EM}$ is the fine-structure constant, $\beta = \sqrt{1-4m^2_\Lambda/q^2}$ the Λ velocity, m_Λ the Λ mass, and $\tau = q^2/(4m^2_\Lambda)$. The results are presented in Table II, shown in Fig. 1, and have significantly improved precision compared to previous measurements [43].

The form factor ratio $R = R(q^2)$ and phase $\Delta\Phi = \Delta\Phi(q^2)$ are obtained at the five energies with sufficient

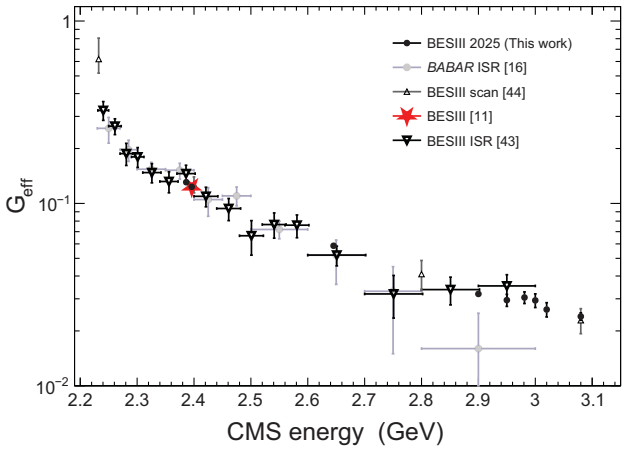

FIG. 1. The effective form factor $G_{\rm eff}$ from this Letter (black dots), BESIII ISR [43], BESIII energy scan [11,44], and *BABAR* ISR [16]. The horizontal error bars denote the bin size.

data. We use a maximum log-likelihood (MLL) fit, where the likelihood function combines the double-tag, single-tag, and background cases (for details, see Refs. [29,38]). In addition, separate fits are carried out for each subsample. We perform bias tests using an ensemble of 1000 MC samples, generated by taking the BESIII detector response and background into account. Each MC sample has the same size as the real data samples. The MLL estimator is found to be unbiased for both R and $\Delta\Phi$ at all subsamples at all energies, except for $\Delta\Phi$ at 2.396 GeV. A detailed MC study found that for 10% of the single-tag Λ samples, the likelihood function does not have a clear maximum, and instead, the MLL fitter assigns a phase $\Delta\Phi = 90°$ regardless of the input value. The likelihood function obtained from the real single-tag Λ sample at 2.396 GeV was found to have the same peculiar shape, in contrast to that of all other samples. Therefore, the $\Delta\Phi$ at this energy is determined only from double-tag $\Lambda\bar{\Lambda}$ and single-tag $\bar{\Lambda}$ events. The R and $\Delta\Phi$ at all other energies are determined using all three samples. The results are shown in Table II and Fig. 2.

A surprising result is that while R is fairly constant, the phase $\Delta\Phi$ increases by about 90° between 2.396 and 2.645 GeV. We perform an independent test where we exploit the $\Lambda\bar{\Lambda}$ spin correlations $C_{\bar{x}z} = C_{\bar{z}x}$ [45], which depend explicitly on $\cos\Delta\Phi$. By calculating these correlations in each hemisphere of the Λ scattering angle and comparing to the prediction for each phase hypothesis, we confirm that $\Delta\Phi$ indeed is below 90° at 2.396 GeV and above 90° at 2.645 and 2.9 GeV.

Systematic effects are investigated by varying all selection criteria for all samples. In most cases the effects are negligible, except for the $M(p\pi)$ window that slightly influences $\Delta\Phi$, and the requirement on the χ^2 from the vertex fit that has a small impact on R. In addition, there is an uncertainty in the $\Lambda/\bar{\Lambda}$ reconstruction efficiency for both R and $\Delta\Phi$. Background effects are studied by sampling MC data mimicking the sideband events in real data. These

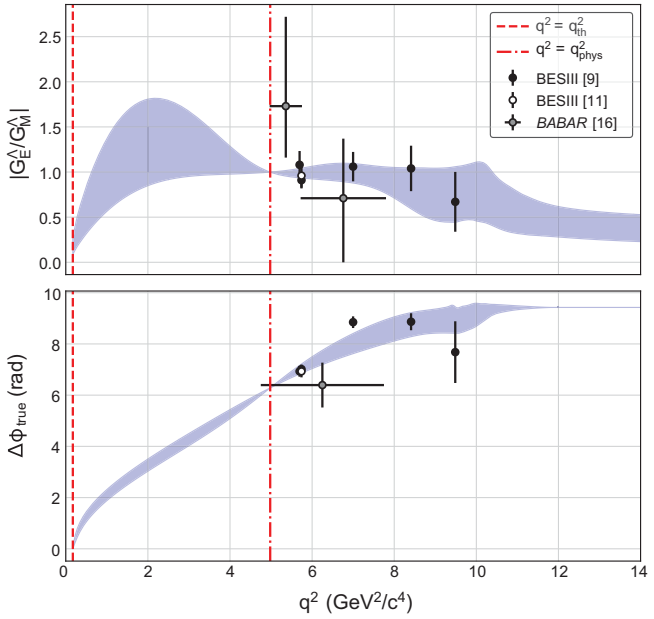

FIG. 2. Top: the modulus $R = |G_E/G_M|$ from this Letter (black dots), from a previous BESIII study (white dot) [11] and from *BABAR* (gray dots) [16]. The band represents a theoretical analysis outlined in Ref. [9], showing the most probable scenario $[N_{\rm th}, N_{\rm asy}] = [0, 3]$. The BESIII 2019 data point is superseded by the point at the same c.m.s. energy in this Letter and is therefore not included in the fit. The red dashed line marks the theoretical threshold $q^2_{\rm th}$, and the red dashed-dotted line the physical threshold $q^2_{\rm phys}$. Bottom: the corresponding measurements of the relative phase $\Delta\Phi$.

background samples are added to signal MC events in 1000 MLL fits. We find the effect to be small, though slightly larger for R than for $\Delta\Phi$. The systematic uncertainties of R and $\Delta\Phi$ are summarized in Table III.

The true phase can be the quoted value plus any integer multiple of 2π, i.e., $\Delta\Phi_{\rm true} = \Delta\Phi + 2\pi N$. However, the dispersive approach in Ref. [9] can help to resolve this ambiguity. Calculations are performed for different scenarios for the quantities

$$N_{\rm th} = \frac{1}{\pi}\arg\left(\frac{G_E(q^2_{\rm th})}{G_M(q^2_{\rm th})}\right), \qquad N_{\rm asy} = \frac{1}{\pi}\arg\left(\frac{G_E(q^2_{\rm asy})}{G_M(q^2_{\rm asy})}\right), \quad (5)$$

where $q^2_{\rm th}$ corresponds to the squared mass of the lowest-lying hadronic state that can couple to the virtual photon and the $\Lambda\bar{\Lambda}$ final state, i.e., $\pi^+\pi^-\pi^0$, and $q^2_{\rm asy}$ is the scale where the phase $\Delta\Phi(q^2)$ approaches an integer multiple of π. At the physical threshold $q^2_{\rm phys} = 4m^2_\Lambda$, only s waves can contribute to the $\Lambda\bar{\Lambda}$ production, and therefore $R(q^2_{\rm phys}) \stackrel{!}{=} 1$ and $\Delta\Phi(q^2_{\rm phys}) \stackrel{!}{=} 2k\pi$. The number of zero-crossings of the complex ratio $G_E(q^2)/G_M(q^2)$ is given by $\Delta N = N_{\rm asy} - N_{\rm th}$, following Cauchy's argument principle. In the calculations, the imaginary part of the ratio is parametrized by Chebyshev polynomials of the first kind. Seven or eight degrees appear optimal and give consistent results as shown in Table IV. The χ^2/ν is obtained from the best fit result. To calculate the probability, we perform simulations of pseudoexperiments of different $[N_{\rm th}, N_{\rm asy}]$ scenarios, using the measured values and their uncertainties as input. The probability P is given by the relative occurrence of a $[N_{\rm th}, N_{\rm asy}]$ scenario for a large number of pseudoexperiments. The most probable scenario, $[N_{\rm th}, N_{\rm asy}] = [0, 3]$ ($P = 85\%$) shown in Fig. 2, is strikingly more probable than the second scenario $[N_{\rm th}, N_{\rm asy}] = [0, 4]$. Notably, all possible solutions imply multiple zero-crossings of $G_E(q^2)/G_M(q^2)$, in line with Dyson-Schwinger-based predictions for nucleons [4] and vector mesons [46].

TABLE III. Systematic uncertainties in R ($\Delta\Phi$) in % at each c.m.s. energy (GeV). The sources are from (I) the $M(p\pi)$ window, (II) vertex fit χ^2 requirement, (III) $\Lambda/\bar{\Lambda}$ reconstruction efficiency, and (IV) background effects.

Source	2.3864	2.3960	2.6454	2.9000	3.0800
(I)	0 (3.7)	0 (3.6)	0 (1.9)	0 (0)	0 (0)
(II)	1.6 (0)	1.6 (0)	0.8 (0)	0 (0)	0 (0)
(III)	1.8 (0.5)	0.7 (0.6)	1.9 (0.2)	1.9 (0.1)	4.5 (2.6)
(IV)	1.6 (0.6)	1.6 (0.6)	1.8 (1.0)	2.0 (1.5)	2.1 (1.8)
Total	2.9 (3.8)	2.4 (3.7)	2.7 (2.2)	2.8 (1.5)	5.0 (3.2)

The sign-normalized rms charge radius is defined as

$$\bar{r}^\Lambda_E = \mathrm{sgn}(\langle r^\Lambda_E\rangle^2)\sqrt{|\langle r^\Lambda_E\rangle^2|}. \quad (6)$$

For neutral baryons with an anomalous magnetic moment, $\langle r^\Lambda_E\rangle^2$ can be calculated from the derivative of $R(q^2)$ at $q^2 = 0$ [9]. The results are presented in Table IV, including the probability of each solution as calculated using Monte Carlo simulations [9]. The most probable $[N_{\rm th}, N_{\rm asy}]$ scenario indicates a negative rms charge radius ($\bar{r}^\Lambda_E = -0.076 \pm 0.043$ fm for a seven degree polynomial). The effect is $\approx$2 standard deviations, and the conclusion is valid also when lower degree polynomials are used in the fit. This indicates that the negative sd quark pair in the Λ is close to the center of the Λ, similar to the dd pair in the

TABLE IV. The rms charge radius $\bar{r}^\Lambda_E$ (in fm) and the probability P (in %) for different $(N_{\rm th}, N_{\rm asy})$ scenarios, obtained by fitting Chebyshev polynomials of the 6th, 7th, and 8th order [9] to data from this Letter and Ref. [16].

	6th, $\chi^2/\nu = 2.5$		7th, $\chi^2/\nu = 1.9$		8th, $\chi^2/\nu = 1.9$	
$(N_{\rm th}, N_{\rm asy})$	$\bar{r}^\Lambda_E$	P	$\bar{r}^\Lambda_E$	P	$\bar{r}^\Lambda_E$	P
(0,3)	−0.125 (70)	57	−0.076 (43)	83	−0.077 (40)	85
(0,4)	−0.109 (62)	26	−0.040 (30)	12	−0.040 (30)	7.6
(1,3)	0.070 (30)	8.0	0.031 (06)	3.0	0.055 (28)	3.8
(−1, 1)	0.152 (59)	5.0	0.025 (19)	1.0	0.019 (16)	1.0

neutron [47]. In summary, our measurements of timelike EMFFs, combined with dispersive relations, open new avenues to study the properties of unstable matter containing strange quarks and beyond.

Acknowledgments—The BESIII Collaboration thanks the staff of BEPCII [48] and the IHEP computing center for their strong support. This work is supported in part by National Key R&D Program of China under Contracts No. 2020YFA0406300, No. 2020YFA0406400, and No. 2023YFA1606000; National Natural Science Foundation of China (NSFC) under Contracts No. 11635010, No. 11735014, No. 11935015, No. 11935016, No. 11935018, No. 12025502, No. 12035009, No. 12035013, No. 12061131003, No. 12192260, No. 12192261, No. 12192262, No. 12192263, No. 12192264, No. 12192265, No. 12221005, No. 12225509, No. 12235017, and No. 12361141819; the Chinese Academy of Sciences (CAS) Large-Scale Scientific Facility Program; the CAS Center for Excellence in Particle Physics (CCEPP); Joint Large-Scale Scientific Facility Funds of the NSFC and CAS under Contract No. U1832207; CAS under Contract No. YSBR-101; 100 Talents Program of CAS; The Institute of Nuclear and Particle Physics (INPAC) and Shanghai Key Laboratory for Particle Physics and Cosmology; German Research Foundation DFG under Contract No. FOR5327; Istituto Nazionale di Fisica Nucleare, Italy; Knut and Alice Wallenberg Foundation under Contracts No. 2021.0174 and No. 2021.0299; Ministry of Development of Turkey under Contract No. DPT2006K-120470; National Research Foundation of Korea under Contract No. NRF-2022R1A2C1092335; National Science and Technology fund of Mongolia; National Science Research and Innovation Fund (NSRF) via the Program Management Unit for Human Resources & Institutional Development, Research and Innovation of Thailand under Contract No. B50G670107; Polish National Science Centre under Contract No. 2019/35/O/ST2/02907; Swedish Research Council under Contracts No. 2019.04595 and No. 2021.04567; The Swedish Foundation for International Cooperation in Research and Higher Education under Contract No. CH2018-7756; U.S. Department of Energy under Contract No. DE-FG02-05ER41374.

Data availability—The data that support the findings of this article are not publicly available upon publication because it is not technically feasible and/or the cost of preparing, depositing, and hosting the data would be prohibitive within the terms of this research project. The data are available from the authors upon reasonable request.

[1] V. Punjabi, C. F. Perdrisat, M. K. Jones, E. J. Brash, and C. E. Carlson, Eur. Phys. J. A **51**, 79 (2015).
[2] S. Pacetti, R. Baldini Ferroli, and E. Tomasi-Gustafsson, Phys. Rep. **550–551**, 1 (2015).
[3] H. Gao and M. Vanderhaeghen, Rev. Mod. Phys. **94**, 015002 (2022).
[4] J. Segovia, I. C. Cloet, C. D. Roberts, and S. M. Schmidt, Few Body Syst. **55**, 1185 (2014).
[5] C. D. Roberts, Symmetry **12**, 1468 (2020).
[6] A. J. R. Puckett *et al.*, Phys. Rev. C **96**, 055203 (2017); **98**, 019907(E) (2018).
[7] G. D. Cates, C. W. de Jager, S. Riordan, and B. Wojtsekhowski, Phys. Rev. Lett. **106**, 252003 (2011).
[8] I. M. Gough Eschrich *et al.* (SELEX Collaboration), Phys. Lett. B **522**, 233 (2001).
[9] A. Mangoni, S. Pacetti, and E. Tomasi-Gustafsson, Phys. Rev. D **104**, 116016 (2021).
[10] A. Z. Dubnickova, S. Dubnicka, and M. P. Rekalo, Nuovo Cimento Soc. Ital. Fis. **109A**, 241 (1996).
[11] M. Ablikim *et al.* (BESIII Collaboration), Phys. Rev. Lett. **123**, 122003 (2019).
[12] J. Haidenbauer, U.-G. Meißner, and L.-Y. Dai, Phys. Rev. D **103**, 014028 (2021).
[13] Y. Yang, D.-Y. Chen, and Z. Lu, Phys. Rev. D **100**, 073007 (2019).
[14] G. Ramalho, M. T. Peña, and K. Tsushima, Phys. Rev. D **101**, 014014 (2020).
[15] Y.-H. Lin, H.-W. Hammer, and U.-G. Meißner, Eur. Phys. J. C **82**, 1091 (2022).
[16] B. Aubert *et al.* (*BABAR* Collaboration), Phys. Rev. D **76**, 092006 (2007).
[17] M. Ablikim *et al.* (BESIII Collaboration), Phys. Rev. Lett. **124**, 042001 (2020).
[18] M. Ablikim *et al.* (BESIII Collaboration), Nat. Phys. **17**, 1200 (2021).
[19] M. Ablikim *et al.* (BESIII Collaboration), Phys. Rev. Lett. **130**, 151905 (2023).
[20] M. Ablikim *et al.* (BESIII Collaboration), Phys. Lett. B **814**, 136110 (2021).
[21] M. Ablikim *et al.* (BESIII Collaboration), Phys. Lett. B **831**, 137187 (2022).
[22] M. Ablikim *et al.* (BESIII Collaboration), Phys. Rev. D **109**, 012002 (2024).
[23] M. Ablikim *et al.* (BESIII Collaboration), Phys. Rev. Lett. **124**, 032002 (2020).
[24] M. Ablikim *et al.* (BESIII Collaboration), Phys. Lett. B **820**, 136557 (2021).
[25] M. Ablikim *et al.* (BESIII Collaboration), Phys. Rev. D **103**, 012005 (2021).
[26] M. Ablikim *et al.* (BESIII Collaboration), Phys. Rev. Lett. **132**, 081904 (2024).
[27] M. Ablikim *et al.* (BESIII Collaboration), Nucl. Instrum. Methods Phys. Res., Sect. A **614**, 345 (2010).
[28] G. Fäldt and A. Kupsc, Phys. Lett. B **772**, 16 (2017).
[29] V. Thorén, Hadron physics in a polarized world: Exploring electromagnetic interactions with spin observables, Ph. D. thesis, Uppsala University, 2022.
[30] BESIII Collaboration, Nat. Phys. **15**, 631 (2019).
[31] M. Ablikim *et al.* (BESIII Collaboration), Nature (London) **606**, 64 (2022).
[32] M. Ablikim *et al.* (BESIII Collaboration), Phys. Rev. Lett. **129**, 131801 (2022).

[33] M. Ablikim *et al.* (BESIII Collaboration), Phys. Rev. D **108**, L031106 (2023).
[34] D. G. Ireland, M. Döring, D. I. Glazier, J. Haidenbauer, M. Mai, R. Murray-Smith, and D. Rönchen, Phys. Rev. Lett. **123**, 182301 (2019).
[35] R. L. Workman and Others (Particle Data Group), Prog. Theor. Exp. Phys. **2022**, 083C01 (2022).
[36] R.-G. Ping, Chin. Phys. C **38**, 083001 (2014).
[37] D. J. Lange, Nucl. Instrum. Methods Phys. Res., Sect. A **462**, 152 (2001).
[38] See Supplemental Material at http://link.aps.org/supplemental/10.1103/9f1h-fl4k for Unraveling the structure of Λ hyperons with polarized $\Lambda\bar{\Lambda}$ pairs.
[39] M. Ablikim *et al.* (BESIII Collaboration), Phys. Rev. D **104**, L091104 (2021).
[40] R.-G. Ping, X.-A. Xiong, L. Xia, Z. Gao, Y.-T. Li, X.-Y. Zhou, B.-X. Zhang, B. Zheng, W.-B. Yan, H.-M. Hu, and G.-S. Huang, Chin. Phys. C **40**, 113002 (2016).
[41] M. Ablikim *et al.* (BESIII Collaboration), Phys. Rev. D **97**, 032013 (2018).
[42] M. Ablikim *et al.* (BESIII Collaboration), Chin. Phys. C **41**, 063001 (2017).
[43] M. Ablikim *et al.* (BESIII Collaboration), Phys. Rev. D **107**, 072005 (2023).
[44] M. Ablikim *et al.* (BESIII Collaboration), Phys. Rev. D **97**, 032013 (2018).
[45] G. Barucca *et al.* (PANDA Collaboration), Eur. Phys. J. A **57**, 154 (2021).
[46] Y.-Z. Xu, D. Binosi, Z.-F. Cui, B.-L. Li, C. D. Roberts, S.-S. Xu, and H. S. Zong, Phys. Rev. D **100**, 114038 (2019).
[47] H. Atac, M. Constantinou, Z. E. Meziani, M. Paolone, and N. Sparveris, Nat. Commun. **12**, 1759 (2021).
[48] https://cstr.cn/31109.02.BEPC.

M. Ablikim,[1] M. N. Achasov,[4,c] P. Adlarson,[76] X. C. Ai,[81] R. Aliberti,[35] A. Amoroso,[75a,75c] Q. An,[72,58,a] Y. Bai,[57] O. Bakina,[36] Y. Ban,[46,h] H.-R. Bao,[64] V. Batozskaya,[1,44] K. Begzsuren,[32] N. Berger,[35] M. Berlowski,[44] M. Bertani,[28a] D. Bettoni,[29a] F. Bianchi,[75a,75c] E. Bianco,[75a,75c] J. Biernat,[76] A. Bortone,[75a,75c] I. Boyko,[36] R. A. Briere,[5] A. Brueggemann,[69] H. Cai,[77] M. H. Cai,[38,k,l] X. Cai,[1,58] A. Calcaterra,[28a] G. F. Cao,[1,64] N. Cao,[1,64] S. A. Cetin,[62a] X. Y. Chai,[46,h] J. F. Chang,[1,58] G. R. Che,[43] Y. Z. Che,[1,58,64] G. Chelkov,[36,b] C. H. Chen,[9] Chao Chen,[55] G. Chen,[1] H. S. Chen,[1,64] H. Y. Chen,[20] M. L. Chen,[1,58,64] S. J. Chen,[42] S. L. Chen,[45] S. M. Chen,[61] T. Chen,[1,64] X. R. Chen,[31,64] X. T. Chen,[1,64] Y. B. Chen,[1,58] Y. Q. Chen,[34] Z. J. Chen,[25,i] Z. K. Chen,[59] S. K. Choi,[10] X. Chu,[12,g] G. Cibinetto,[29a] F. Cossio,[75c] J. J. Cui,[50] H. L. Dai,[1,58] J. P. Dai,[79] A. Dbeyssi,[18] R. E. de Boer,[3] D. Dedovich,[36] C. Q. Deng,[73] Z. Y. Deng,[1] A. Denig,[35] I. Denysenko,[36] M. Destefanis,[75a,75c] F. De Mori,[75a,75c] B. Ding,[67,1] X. X. Ding,[46,h] Y. Ding,[40] Y. Ding,[34] Y. X. Ding,[30] J. Dong,[1,58] L. Y. Dong,[1,64] M. Y. Dong,[1,58,64] X. Dong,[77] M. C. Du,[1] S. X. Du,[12,g] S. X. Du,[81] Y. Y. Duan,[55] Z. H. Duan,[42] P. Egorov,[36,b] G. F. Fan,[42] J. J. Fan,[19] Y. H. Fan,[45] J. Fang,[1,58] J. Fang,[59] S. S. Fang,[1,64] W. X. Fang,[1] Y. Q. Fang,[1,58] R. Farinelli,[29a] L. Fava,[75b,75c] F. Feldbauer,[3] G. Felici,[28a] C. Q. Feng,[72,58] J. H. Feng,[59] Y. T. Feng,[72,58] M. Fritsch,[3] C. D. Fu,[1] J. L. Fu,[64] Y. W. Fu,[1,64] H. Gao,[64] X. B. Gao,[41] Y. N. Gao,[19] Y. N. Gao,[46,h] Y. Y. Gao,[30] Yang Gao,[72,58] S. Garbolino,[75c] I. Garzia,[29a,29b] P. T. Ge,[19] Z. W. Ge,[42] C. Geng,[59] E. M. Gersabeck,[68] A. Gilman,[70] K. Goetzen,[13] J. D. Gong,[34] L. Gong,[40] W. X. Gong,[1,58] W. Gradl,[35] S. Gramigna,[29a,29b] M. Greco,[75a,75c] M. H. Gu,[1,58] Y. T. Gu,[15] C. Y. Guan,[1,64] A. Q. Guo,[31] L. B. Guo,[41] M. J. Guo,[50] R. P. Guo,[49] Y. P. Guo,[12,g] A. Guskov,[36,b] J. Gutierrez,[27] K. L. Han,[64] T. T. Han,[1] F. Hanisch,[3] K. D. Hao,[72,58] X. Q. Hao,[19] F. A. Harris,[66] K. K. He,[55] K. L. He,[1,64] F. H. Heinsius,[3] C. H. Heinz,[35] Y. K. Heng,[1,58,64] C. Herold,[60] T. Holtmann,[3] P. C. Hong,[34] G. Y. Hou,[1,64] X. T. Hou,[1,64] Y. R. Hou,[64] Z. L. Hou,[1] H. M. Hu,[1,64] J. F. Hu,[56,j] Q. P. Hu,[72,58] S. L. Hu,[12,g] T. Hu,[1,58,64] Y. Hu,[1] Z. M. Hu,[59] G. S. Huang,[72,58] K. X. Huang,[59] L. Q. Huang,[31,64] P. Huang,[42] X. T. Huang,[50] Y. P. Huang,[1] Y. S. Huang,[59] T. Hussain,[74] N. Hüsken,[35] N. in der Wiesche,[69] J. Jackson,[27] S. Janchiv,[32] Q. Ji,[1] Q. P. Ji,[19] W. Ji,[1,64] X. B. Ji,[1,64] X. L. Ji,[1,58] Y. Y. Ji,[50] Z. K. Jia,[72,58] D. Jiang,[1,64] H. B. Jiang,[77] P. C. Jiang,[46,h] S. J. Jiang,[9] T. J. Jiang,[16] X. S. Jiang,[1,58,64] Y. Jiang,[64] J. B. Jiao,[50] J. K. Jiao,[34] Z. Jiao,[23] S. Jin,[42] Y. Jin,[67] M. Q. Jing,[1,64] X. M. Jing,[64] T. Johansson,[76] S. Kabana,[33] N. Kalantar-Nayestanaki,[65] X. L. Kang,[9] X. S. Kang,[40] M. Kavatsyuk,[65] B. C. Ke,[81] V. Khachatryan,[27] A. Khoukaz,[69] R. Kiuchi,[1] O. B. Kolcu,[62a] B. Kopf,[3] M. Kuessner,[3] X. Kui,[1,64] N. Kumar,[26] A. Kupsc,[44,76] W. Kühn,[37] Q. Lan,[73] W. N. Lan,[19] T. T. Lei,[72,58] M. Lellmann,[35] T. Lenz,[35] C. Li,[43] C. Li,[47] C. H. Li,[39] C. K. Li,[20] Cheng Li,[72,58] D. M. Li,[81] F. Li,[1,58] G. Li,[1] H. B. Li,[1,64] H. J. Li,[19] H. N. Li,[56,j] Hui Li,[43] J. R. Li,[61] J. S. Li,[59] K. Li,[1] K. L. Li,[19] K. L. Li,[38,k,l] L. J. Li,[1,64] Lei Li,[48] M. H. Li,[43] M. R. Li,[1,64] P. L. Li,[64] P. R. Li,[38,k,l] Q. M. Li,[1,64] Q. X. Li,[50] R. Li,[17,31] T. Li,[50] T. Y. Li,[43] W. D. Li,[1,64] W. G. Li,[1,a] X. Li,[1,64] X. H. Li,[72,58] X. L. Li,[50] X. Y. Li,[1,8] X. Z. Li,[59] Y. Li,[19] Y. G. Li,[46,h] Y. P. Li,[34] Z. J. Li,[59] Z. Y. Li,[79] C. Liang,[42] H. Liang,[72,58] Y. F. Liang,[54] Y. T. Liang,[31,64] G. R. Liao,[14] L. B. Liao,[59] M. H. Liao,[59] Y. P. Liao,[1,64] J. Libby,[26] A. Limphirat,[60] C. C. Lin,[55] C. X. Lin,[64] D. X. Lin,[31,64] L. Q. Lin,[39] T. Lin,[1] B. J. Liu,[1] B. X. Liu,[77] C. Liu,[34]

C. X. Liu,[1] F. Liu,[1] F. H. Liu,[53] Feng Liu,[6] G. M. Liu,[56,j] H. Liu,[38,k,l] H. B. Liu,[15] H. H. Liu,[1] H. M. Liu,[1,64] Huihui Liu,[21] J. B. Liu,[72,58] J. J. Liu,[20] K. Liu,[73] K. Liu,[38,k,l] K. Y. Liu,[40] Ke Liu,[22] L. Liu,[72,58] L. C. Liu,[43] Lu Liu,[43] P. L. Liu,[1] Q. Liu,[64] S. B. Liu,[72,58] T. Liu,[12,g] W. K. Liu,[43] W. M. Liu,[72,58] W. T. Liu,[39] X. Liu,[39] X. Liu,[38,k,l] X. Y. Liu,[77] Y. Liu,[38,k,l] Y. Liu,[81] Y. Liu,[81] Y. B. Liu,[43] Z. A. Liu,[1,58,64] Z. D. Liu,[9] Z. Q. Liu,[50] X. C. Lou,[1,58,64] F. X. Lu,[59] H. J. Lu,[23] J. G. Lu,[1,58] Y. Lu,[7] Y. H. Lu,[1,64] Y. P. Lu,[1,58] Z. H. Lu,[1,64] C. L. Luo,[41] J. R. Luo,[59] J. S. Luo,[1,64] M. X. Luo,[80] T. Luo,[12,g] X. L. Luo,[1,58] Z. Y. Lv,[22] X. R. Lyu,[64,p] Y. F. Lyu,[43] Y. H. Lyu,[81] F. C. Ma,[40] H. Ma,[79] H. L. Ma,[1] J. L. Ma,[1,64] L. L. Ma,[50] L. R. Ma,[67] Q. M. Ma,[1] R. Q. Ma,[1,64] R. Y. Ma,[19] T. Ma,[72,58] X. T. Ma,[1,64] X. Y. Ma,[1,58] Y. M. Ma,[31] F. E. Maas,[18] I. MacKay,[70] M. Maggiora,[75a,75c] S. Malde,[70] Y. J. Mao,[46,h] Z. P. Mao,[1] S. Marcello,[75a,75c] F. M. Melendi,[29a,29b] Y. H. Meng,[64] Z. X. Meng,[67] J. G. Messchendorp,[13,65] G. Mezzadri,[29a] H. Miao,[1,64] T. J. Min,[42] R. E. Mitchell,[27] X. H. Mo,[1,58,64] B. Moses,[27] N. Yu. Muchnoi,[4,c] J. Muskalla,[35] Y. Nefedov,[36] F. Nerling,[18,e] L. S. Nie,[20] I. B. Nikolaev,[4,c] Z. Ning,[1,58] S. Nisar,[11,m] Q. L. Niu,[38,k,l] W. D. Niu,[12,g] S. L. Olsen,[10,64] Q. Ouyang,[1,58,64] S. Pacetti,[28b,28c] X. Pan,[55] Y. Pan,[57] A. Pathak,[10] Y. P. Pei,[72,58] M. Pelizaeus,[3] H. P. Peng,[72,58] Y. Y. Peng,[38,k,l] K. Peters,[13,e] J. L. Ping,[41] R. G. Ping,[1,64] S. Plura,[35] V. Prasad,[33] F. Z. Qi,[1] H. R. Qi,[61] M. Qi,[42] S. Qian,[1,58] W. B. Qian,[64] C. F. Qiao,[64] J. H. Qiao,[19] J. J. Qin,[73] J. L. Qin,[55] L. Q. Qin,[14] L. Y. Qin,[72,58] P. B. Qin,[73] X. P. Qin,[12,g] X. S. Qin,[50] Z. H. Qin,[1,58] J. F. Qiu,[1] Z. H. Qu,[73] C. F. Redmer,[35] A. Rivetti,[75c] M. Rolo,[75c] G. Rong,[1,64] S. S. Rong,[1,64] F. Rosini,[28b,28c] Ch. Rosner,[18] M. Q. Ruan,[1,58] N. Salone,[44] A. Sarantsev,[36,d] Y. Schelhaas,[35] K. Schoenning,[76,q] M. Scodeggio,[29a] K. Y. Shan,[12,g] W. Shan,[24] X. Y. Shan,[72,58] Z. J. Shang,[38,k,l] J. F. Shangguan,[16] L. G. Shao,[1,64] M. Shao,[72,58] C. P. Shen,[12,g] H. F. Shen,[1,8] W. H. Shen,[64] X. Y. Shen,[1,64] B. A. Shi,[64] H. Shi,[72,58] J. L. Shi,[12,g] J. Y. Shi,[1] S. Y. Shi,[73] X. Shi,[1,58] H. L. Song,[72,58] J. J. Song,[19] T. Z. Song,[59] W. M. Song,[34,1] Y. X. Song,[46,h,n] S. Sosio,[75a,75c] S. Spataro,[75a,75c] F. Stieler,[35] S. S. Su,[40] Y. J. Su,[64] G. B. Sun,[77] G. X. Sun,[1] H. Sun,[64] H. K. Sun,[1] J. F. Sun,[19] K. Sun,[61] L. Sun,[77] S. S. Sun,[1,64] T. Sun,[51,f] Y. C. Sun,[77] Y. H. Sun,[30] Y. J. Sun,[72,58] Y. Z. Sun,[1] Z. Q. Sun,[1,64] Z. T. Sun,[50] C. J. Tang,[54] G. Y. Tang,[1] J. Tang,[59] L. F. Tang,[39] M. Tang,[72,58] Y. A. Tang,[77] L. Y. Tao,[73] M. Tat,[70] J. X. Teng,[72,58] J. Y. Tian,[72,58] W. H. Tian,[59] Y. Tian,[31] Z. F. Tian,[77] V. Thoren,[76] I. Uman,[62b] B. Wang,[1] B. Wang,[59] Bo Wang,[72,58] C. Wang,[19] Cong Wang,[22] D. Y. Wang,[46,h] H. J. Wang,[38,k,l] J. J. Wang,[77] K. Wang,[1,58] L. L. Wang,[1] L. W. Wang,[34] M. Wang,[72,58] M. Wang,[50] N. Y. Wang,[64] S. Wang,[12,g] T. Wang,[12,g] T. J. Wang,[43] W. Wang,[59] W. Wang,[73] W. P. Wang,[35,58,72,o] X. Wang,[46,h] X. F. Wang,[38,k,l] X. J. Wang,[39] X. L. Wang,[12,g] X. N. Wang,[1] Y. Wang,[61] Y. D. Wang,[45] Y. F. Wang,[1,58,64] Y. H. Wang,[38,k,l] Y. L. Wang,[19] Y. N. Wang,[77] Y. Q. Wang,[1] Yaqian Wang,[17] Yi Wang,[61] Yuan Wang,[17,31] Z. Wang,[1,58] Z. L. Wang,[2] Z. L. Wang,[73] Z. Q. Wang,[12,g] Z. Y. Wang,[1,64] D. H. Wei,[14] H. R. Wei,[43] F. Weidner,[69] S. P. Wen,[1] Y. R. Wen,[39] U. Wiedner,[3] G. Wilkinson,[70] M. Wolke,[76] C. Wu,[39] J. F. Wu,[1,8] L. H. Wu,[1] L. J. Wu,[1,64] Lianjie Wu,[19] S. G. Wu,[1,64] S. M. Wu,[64] X. Wu,[12,g] X. H. Wu,[34] Y. J. Wu,[31] Z. Wu,[1,58] L. Xia,[72,58] X. M. Xian,[39] B. H. Xiang,[1,64] T. Xiang,[46,h] D. Xiao,[38,k,l] G. Y. Xiao,[42] H. Xiao,[73] Y. L. Xiao,[12,g] Z. J. Xiao,[41] C. Xie,[42] K. J. Xie,[1,64] X. H. Xie,[46,h] Y. Xie,[50] Y. G. Xie,[1,58] Y. H. Xie,[6] Z. P. Xie,[72,58] T. Y. Xing,[1,64] C. F. Xu,[1,64] C. J. Xu,[59] G. F. Xu,[1] H. Y. Xu,[2] H. Y. Xu,[67,2] M. Xu,[72,58] Q. J. Xu,[16] Q. N. Xu,[30] T. D. Xu,[73] W. L. Xu,[67] X. P. Xu,[55] Y. Xu,[40] Y. Xu,[12,g] Y. C. Xu,[78] Z. S. Xu,[64] H. Y. Yan,[39] L. Yan,[12,g] W. B. Yan,[72,58] W. C. Yan,[81] W. P. Yan,[19] X. Q. Yan,[1,64] H. J. Yang,[51,f] H. L. Yang,[34] H. X. Yang,[1] J. H. Yang,[42] R. J. Yang,[19] T. Yang,[1] Y. Yang,[12,g] Y. F. Yang,[43] Y. H. Yang,[42] Y. Q. Yang,[9] Y. X. Yang,[1,64] Y. Z. Yang,[19] M. Ye,[1,58] M. H. Ye,[8] Z. J. Ye,[56,j] Junhao Yin,[43] Z. Y. You,[59] B. X. Yu,[1,58,64] C. X. Yu,[43] G. Yu,[13] J. S. Yu,[25,i] M. C. Yu,[40] T. Yu,[73] X. D. Yu,[46,h] Y. C. Yu,[81] C. Z. Yuan,[1,64] H. Yuan,[1,64] J. Yuan,[34] J. Yuan,[45] L. Yuan,[2] S. C. Yuan,[1,64] Y. Yuan,[1,64] Z. Y. Yuan,[59] C. X. Yue,[39] Ying Yue,[19] A. A. Zafar,[74] S. H. Zeng,[63] X. Zeng,[12,g] Y. Zeng,[25,i] Y. J. Zeng,[1,64] Y. J. Zeng,[59] X. Y. Zhai,[34] Y. H. Zhan,[59] A. Q. Zhang,[1,64] B. L. Zhang,[1,64] B. X. Zhang,[1] D. H. Zhang,[43] G. Y. Zhang,[19] G. Y. Zhang,[1,64] H. Zhang,[72,58] H. Zhang,[81] H. C. Zhang,[1,58,64] H. H. Zhang,[59] H. Q. Zhang,[1,58,64] H. R. Zhang,[72,58] H. Y. Zhang,[1,58] J. Zhang,[59] J. Zhang,[81] J. J. Zhang,[52] J. L. Zhang,[20] J. Q. Zhang,[41] J. S. Zhang,[12,g] J. W. Zhang,[1,58,64] J. X. Zhang,[38,k,l] J. Y. Zhang,[1] J. Z. Zhang,[1,64] Jianyu Zhang,[64] L. M. Zhang,[61] Lei Zhang,[42] N. Zhang,[81] P. Zhang,[1,64] Q. Zhang,[19] Q. Y. Zhang,[34] R. Y. Zhang,[38,k,l] S. H. Zhang,[1,64] Shulei Zhang,[25,i] X. M. Zhang,[1] X. Y. Zhang,[40] X. Y. Zhang,[50] Y. Zhang,[73] Y. Zhang,[1] Y. T. Zhang,[81] Y. H. Zhang,[1,58] Y. M. Zhang,[39] Z. D. Zhang,[1] Z. H. Zhang,[1] Z. L. Zhang,[34] Z. L. Zhang,[55] Z. X. Zhang,[19] Z. Y. Zhang,[77] Z. Y. Zhang,[43] Z. Z. Zhang,[45] Zh. Zh. Zhang,[19] G. Zhao,[1] J. Y. Zhao,[1,64] J. Z. Zhao,[1,58] L. Zhao,[1] Lei Zhao,[72,58] M. G. Zhao,[43] N. Zhao,[79] R. P. Zhao,[64] S. J. Zhao,[81] Y. B. Zhao,[1,58] Y. L. Zhao,[55] Y. X. Zhao,[31,64] Z. G. Zhao,[72,58] A. Zhemchugov,[36,b] B. Zheng,[73] B. M. Zheng,[34] J. P. Zheng,[1,58] W. J. Zheng,[1,64] X. R. Zheng,[19] Y. H. Zheng,[64,p] B. Zhong,[41] H. Zhou,[35,50,o] J. Q. Zhou,[34]

J. Y. Zhou,[34] S. Zhou,[6] X. Zhou,[77] X. K. Zhou,[6] X. R. Zhou,[72,58] X. Y. Zhou,[39] Y. Z. Zhou,[12,g] Z. C. Zhou,[20] A. N. Zhu,[64] J. Zhu,[43] K. Zhu,[1] K. J. Zhu,[1,58,64] K. S. Zhu,[12,g] L. Zhu,[34] L. X. Zhu,[64] S. H. Zhu,[71] T. J. Zhu,[12,g] W. D. Zhu,[12,g] W. D. Zhu,[41] W. J. Zhu,[1] W. Z. Zhu,[19] Y. C. Zhu,[72,58] Z. A. Zhu,[1,64] X. Y. Zhuang,[43] J. H. Zou,[1] and J. Zu[72,58]

(BESIII Collaboration)

[1]*Institute of High Energy Physics, Beijing 100049, People's Republic of China*
[2]*Beihang University, Beijing 100191, People's Republic of China*
[3]*Bochum Ruhr-University, D-44780 Bochum, Germany*
[4]*Budker Institute of Nuclear Physics SB RAS (BINP), Novosibirsk 630090, Russia*
[5]*Carnegie Mellon University, Pittsburgh, Pennsylvania 15213, USA*
[6]*Central China Normal University, Wuhan 430079, People's Republic of China*
[7]*Central South University, Changsha 410083, People's Republic of China*
[8]*China Center of Advanced Science and Technology, Beijing 100190, People's Republic of China*
[9]*China University of Geosciences, Wuhan 430074, People's Republic of China*
[10]*Chung-Ang University, Seoul 06974, Republic of Korea*
[11]*COMSATS University Islamabad, Lahore Campus, Defence Road, Off Raiwind Road, 54000 Lahore, Pakistan*
[12]*Fudan University, Shanghai 200433, People's Republic of China*
[13]*GSI Helmholtzcentre for Heavy Ion Research GmbH, D-64291 Darmstadt, Germany*
[14]*Guangxi Normal University, Guilin 541004, People's Republic of China*
[15]*Guangxi University, Nanning 530004, People's Republic of China*
[16]*Hangzhou Normal University, Hangzhou 310036, People's Republic of China*
[17]*Hebei University, Baoding 071002, People's Republic of China*
[18]*Helmholtz Institute Mainz, Staudinger Weg 18, D-55099 Mainz, Germany*
[19]*Henan Normal University, Xinxiang 453007, People's Republic of China*
[20]*Henan University, Kaifeng 475004, People's Republic of China*
[21]*Henan University of Science and Technology, Luoyang 471003, People's Republic of China*
[22]*Henan University of Technology, Zhengzhou 450001, People's Republic of China*
[23]*Huangshan College, Huangshan 245000, People's Republic of China*
[24]*Hunan Normal University, Changsha 410081, People's Republic of China*
[25]*Hunan University, Changsha 410082, People's Republic of China*
[26]*Indian Institute of Technology Madras, Chennai 600036, India*
[27]*Indiana University, Bloomington, Indiana 47405, USA*
[28a]*INFN Laboratori Nazionali di Frascati, INFN Laboratori Nazionali di Frascati, I-00044 Frascati, Italy*
[28b]*INFN Sezione di Perugia, I-06100 Perugia, Italy*
[28c]*University of Perugia, I-06100 Perugia, Italy*
[29a]*INFN Sezione di Ferrara, INFN Sezione di Ferrara, I-44122 Ferrara, Italy*
[29b]*University of Ferrara, I-44122 Ferrara, Italy*
[30]*Inner Mongolia University, Hohhot 010021, People's Republic of China*
[31]*Institute of Modern Physics, Lanzhou 730000, People's Republic of China*
[32]*Institute of Physics and Technology, Mongolian Academy of Sciences, Peace Avenue 54B, Ulaanbaatar 13330, Mongolia*
[33]*Instituto de Alta Investigación, Universidad de Tarapacá, Casilla 7D, Arica 1000000, Chile*
[34]*Jilin University, Changchun 130012, People's Republic of China*
[35]*Johannes Gutenberg University of Mainz, Johann-Joachim-Becher-Weg 45, D-55099 Mainz, Germany*
[36]*Joint Institute for Nuclear Research, 141980 Dubna, Moscow region, Russia*
[37]*Justus-Liebig-Universitaet Giessen, II. Physikalisches Institut, Heinrich-Buff-Ring 16, D-35392 Giessen, Germany*
[38]*Lanzhou University, Lanzhou 730000, People's Republic of China*
[39]*Liaoning Normal University, Dalian 116029, People's Republic of China*
[40]*Liaoning University, Shenyang 110036, People's Republic of China*
[41]*Nanjing Normal University, Nanjing 210023, People's Republic of China*
[42]*Nanjing University, Nanjing 210093, People's Republic of China*
[43]*Nankai University, Tianjin 300071, People's Republic of China*
[44]*National Centre for Nuclear Research, Warsaw 02-093, Poland*
[45]*North China Electric Power University, Beijing 102206, People's Republic of China*
[46]*Peking University, Beijing 100871, People's Republic of China*

[47]Qufu Normal University, Qufu 273165, People's Republic of China
[48]Renmin University of China, Beijing 100872, People's Republic of China
[49]Shandong Normal University, Jinan 250014, People's Republic of China
[50]Shandong University, Jinan 250100, People's Republic of China
[51]Shanghai Jiao Tong University, Shanghai 200240, People's Republic of China
[52]Shanxi Normal University, Linfen 041004, People's Republic of China
[53]Shanxi University, Taiyuan 030006, People's Republic of China
[54]Sichuan University, Chengdu 610064, People's Republic of China
[55]Soochow University, Suzhou 215006, People's Republic of China
[56]South China Normal University, Guangzhou 510006, People's Republic of China
[57]Southeast University, Nanjing 211100, People's Republic of China
[58]State Key Laboratory of Particle Detection and Electronics, Beijing 100049, Hefei 230026, People's Republic of China
[59]Sun Yat-Sen University, Guangzhou 510275, People's Republic of China
[60]Suranaree University of Technology, University Avenue 111, Nakhon Ratchasima 30000, Thailand
[61]Tsinghua University, Beijing 100084, People's Republic of China
[62a]Turkish Accelerator Center Particle Factory Group, Istinye University, 34010, Istanbul, Turkey
[62b]Near East University, Nicosia, North Cyprus, 99138, Mersin 10, Turkey
[63]University of Bristol, H H Wills Physics Laboratory, Tyndall Avenue, Bristol, BS8 1TL, United Kingdom
[64]University of Chinese Academy of Sciences, Beijing 100049, People's Republic of China
[65]University of Groningen, NL-9747 AA Groningen, The Netherlands
[66]University of Hawaii, Honolulu, Hawaii 96822, USA
[67]University of Jinan, Jinan 250022, People's Republic of China
[68]University of Manchester, Oxford Road, Manchester, M13 9PL, United Kingdom
[69]University of Muenster, Wilhelm-Klemm-Strasse 9, 48149 Muenster, Germany
[70]University of Oxford, Keble Road, Oxford OX13RH, United Kingdom
[71]University of Science and Technology Liaoning, Anshan 114051, People's Republic of China
[72]University of Science and Technology of China, Hefei 230026, People's Republic of China
[73]University of South China, Hengyang 421001, People's Republic of China
[74]University of the Punjab, Lahore-54590, Pakistan
[75a]University of Turin and INFN, University of Turin, I-10125 Turin, Italy
[75b]University of Eastern Piedmont, I-15121 Alessandria, Italy
[75c]INFN, I-10125 Turin, Italy
[76]Uppsala University, Box 516, SE-75120 Uppsala, Sweden
[77]Wuhan University, Wuhan 430072, People's Republic of China
[78]Yantai University, Yantai 264005, People's Republic of China
[79]Yunnan University, Kunming 650500, People's Republic of China
[80]Zhejiang University, Hangzhou 310027, People's Republic of China
[81]Zhengzhou University, Zhengzhou 450001, People's Republic of China

[a]Deceased.
[b]Also at the Moscow Institute of Physics and Technology, Moscow 141700, Russia.
[c]Also at the Novosibirsk State University, Novosibirsk 630090, Russia.
[d]Also at the NRC "Kurchatov Institute," PNPI, 188300 Gatchina, Russia.
[e]Also at Goethe University Frankfurt, 60323 Frankfurt am Main, Germany.
[f]Also at Key Laboratory for Particle Physics, Astrophysics and Cosmology, Ministry of Education, Shanghai Key Laboratory for Particle Physics and Cosmology, Institute of Nuclear and Particle Physics, Shanghai 200240, People's Republic of China.
[g]Also at Key Laboratory of Nuclear Physics and Ion-beam Application (MOE) and Institute of Modern Physics, Fudan University, Shanghai 200443, People's Republic of China.
[h]Also at State Key Laboratory of Nuclear Physics and Technology, Peking University, Beijing 100871, People's Republic of China.
[i]Also at School of Physics and Electronics, Hunan University, Changsha 410082, China.
[j]Also at Guangdong Provincial Key Laboratory of Nuclear Science, Institute of Quantum Matter, South China Normal University, Guangzhou 510006, China.
[k]Also at MOE Frontiers Science Center for Rare Isotopes, Lanzhou University, Lanzhou 730000, People's Republic of China.
[l]Also at Lanzhou Center for Theoretical Physics, Lanzhou University, Lanzhou 730000, People's Republic of China.
[m]Also at the Department of Mathematical Sciences, IBA, Karachi 75270, Pakistan.
[n]Also at Ecole Polytechnique Federale de Lausanne (EPFL), CH-1015 Lausanne, Switzerland.
[o]Also at Helmholtz Institute Mainz, Staudinger Weg 18, D-55099 Mainz, Germany.
[p]Also at Hangzhou Institute for Advanced Study, University of Chinese Academy of Sciences, Hangzhou 310024, China.
[q]Contact author: karin.schonning@physics.uu.se